REFERENCES AND NOTES

1. F. J. Sawkins, *Metal Deposits in Relation to Plate Tectonics* (Springer-Verlag, New York, ed. 2, 1990).
2. P. J. Coney, *Am. J. Sci.* **272**, 603 (1972); in *New Mex. Geol. Soc. Field Conf. Guideb.* **29**, 285 (1978).
3. B. L. Gulson, *Lead Isotopes in Mineral Exploration* (Elsevier, New York, 1986).
4. F. Corfu and T. L. Muir, *Chem. Geol.* **79**, 183 (1989).
5. P. E. Damon *et al.*, *U.S.A.E.C. Annu. Rep. C00-689-42* (1964); R. L. Mauger, P. E. Damon, B. J. Giletti, *Trans. Soc. Min. Eng.* **232**, 81 (1965); D. E. Livingston, R. L. Mauger, P. E. Damon, *Econ. Geol.* **63**, 30 (1968); F. W. McDowell, *Isochron West* **2**, 1 (1971); N. G. Banks *et al.*, *Econ. Geol.* **67**, 861 (1972); S. C. Creasey, *ibid.* **75**, 830 (1980).
6. L. W. Snee, J. F. Sutter, W. C. Kelly, *Econ. Geol.* **83**, 335 (1988).
7. J. T. Chesley *et al.*, *Geochim. Cosmochim. Acta* **57**, 1817 (1993).
8. E. Y. Anthony and S. R. Titley, *Ariz. Geol. Soc. Dig.* **17**, 485 (1989).
9. S. R. Titley, in *Advances in Geology of the Porphyry Copper Deposits, Southwestern North America*, S. R. Titley, Ed. (Univ. of Arizona Press, Tucson, 1982), pp. 353–373.
10. G. L. Farmer, and D. J. DePaolo, *J. Geophys. Res.* **88**, 3379 (1983); V. C. Bennett and D. J. DePaolo, *Geol. Soc. Am. Bull.* **99**, 674 (1987); J. L. Wooden and R. M. Tosdal, *Geol. Soc. Am. Abstr. Programs* **22**, 95 (1990); K. R. Chamberlain and S. A. Bowring, *J. Geol.* **98**, 399 (1990).
11. S. R. Titley, *Geol. Soc. Am. Bull.* **99**, 814 (1987); *Miner. Deposita* **26**, 66 (1991).
12. J. W. Morgan and J. F. Lovering, *Earth Planet. Sci. Lett.* **3**, 219 (1967); R. J. Ford, *J. Geol. Soc. Aust.* **15**, 189 (1968).
13. W. Herr and E. Merz, *Z. Naturforsch. Teil A* **10**, 613 (1955); *ibid.* **13**, 231 (1958); W. Hirt, W. Herr, W. Hoffmeister, *Radioactive Dating* (International Atomic Energy Agency, Vienna, 1963), pp. 35–43; S. Ishihara *et al.*, *Geochem. J.* **23**, 85 (1989); J.-M. Luck and C. J. Allègre, *Earth Planet. Sci. Lett.* **61**, 291 (1982); J.-M. Luck *et al.*, *Eos* **64**, 334 (1983).
14. R. J. Newberry, *Am. Miner.* **64**, 758 (1979).
15. T. E. McCandless, J. Ruiz, A. R. Campbell, *Geochim. Cosmochim. Acta* **57**, 889 (1993).
16. J. W. Morgan and R. J. Walker, *Anal. Chim. Acta.* **222**, 291 (1989).
17. F. W. Warnaars *et al.*, *Econ. Geol.* **73**, 1242 (1978); W. J. Moore, M. A. Lanphere, J. D. Obradovich, *ibid.* **63**, 612 (1968); W. J. Moore and M. A. Lanphere, *ibid.* **66**, 331 (1971).
18. C. A. Anderson, E. A. Sholz, J. D. Strobell, *U.S. Geol. Surv. Prof. Pap. 278* (1955), p. 103.
19. J. R. Lang, thesis, University of Arizona, Tucson (1991).
20. P. K. Medhi, *Ariz. Geol. Soc. Dig.* **11**, 79 (1978).
21. P. E. Damon and R. L. Mauger, *Trans. Soc. Min. Eng.* **235**, 99 (1966).
22. M. Shafiqullah *et al.*, *Ariz. Geol. Soc. Dig.* **12**, 210 (1980).
23. S. C. Creasey and R. Kistler, *U.S. Geol. Surv. Prof. Pap. 450-D* (1962), p. D1; J. G. Guthrie and D. G. Moore, *Ariz. Geol. Soc. Dig.* **11**, 25 (1978).
24. J. R. Velasco, in *Geology of the Porphyry Copper Deposits: Southwestern North America*, S. R. Titley and C. L. Hicks, Eds. (Univ. of Arizona Press, Tucson, 1966), pp. 245–250.
25. T. H. Anderson and L. T. Silver, *Econ. Geol.* **72**, 827 (1977); S. E. Bushnell, *ibid.* **83**, 1760 (1988).
26. W. A. Wodzicki, thesis, University of California, Los Angeles (1992).
27. K. C. Bennett, thesis, University of Arizona, Tucson (1975).
28. J. M. Langton, *Trans. Soc. Min. Eng.* **254**, 24 (1973).
29. S. R. Titley, in (*9*), p. 387.
30. M. Shafiqullah and J. D. Langlois, *New Mex. Geol. Soc. Field Conf. Guideb.* **29**, 321 (1978).
31. For two dated igneous events to be separable in time with greater than 95% confidence, their apparent difference in age must not exceed the critical value

$$1.96\left[\left(\frac{\sigma_1}{n_1}\right)^2 + \left(\frac{\sigma_2}{n_2}\right)^2\right]^{1/2}$$

where σ_1 and σ_2 are the respective standard deviations (in percent) of the ages and n_1 and n_2 are the respective numbers of measurements [G. B. Dalrymple and M. A. Lanphere, *Potassium-Argon Dating* (Freeman, San Francisco, 1969)].
32. R. F. Marvin, T. W. Stern, S. C. Creasey, L. H. Mehnert, *U.S. Geol. Surv. Bull.* **27**, 1379 (1973).
33. S. R. Titley and R. E. Beane, in *Economic Geology 75th Anniversary Volume*, B. J. Skinner, Ed. (Economic Geology, New Haven, CT, 1981), pp. 214–269.
34. W. Hildreth and S. Moorbath, *Contrib. Mineral. Petrol.* **98**, 455 (1988).
35. T. Atwater, *Geol. Soc. Am. Bull.* **81**, 3513 (1970); ——— and H. W. Menard, *Earth Planet. Sci. Lett.* **7**, 445 (1970); D. Jurdy, *Tectonics* **3**, 107 (1984); D. C. Engebretson *et al.*, *ibid.*, p. 115.
36. S. R. Titley and T. L. Heidrick, *Econ. Geol.* **73**, 891 (1978).
37. S. R. Titley *et al.*, *ibid.* **81**, 343 (1986).
38. G. L. Farmer and D. J. DePaolo, *J. Geophys. Res.* **89**, 10141 (1984); E. Y. Anthony and S. R. Titley, *Proceedings of the Seventh Quadrennial International Association for the Genesis of Ore Deposits Symposium* (E. Schweizerbart'sche Verlagsbuchhandlung, Stuttgart, Germany, 1988, pp. 535–546; E. Y. Anthony and S. R. Titley, *Geochim. Cosmochim. Acta.* **52**, 2235 (1990).
39. S. M. F. Sheppard, R. L. Nielsen, H. P. Taylor, Jr., *Econ. Geol.* **66**, 515 (1971); K. B. Krauskopf, *Geochim. Cosmochim. Acta.* **35**, 643 (1971); J. R. Bowman *et al.*, *Econ. Geol.* **82**, 395 (1987); R. M. Bouse, J. Ruiz, S. R. Titley, J. R. Lang, *Eos* **71**, 1681 (1990); J. R. Lang, S. R. Titley, P. J. Patchett, J. Ruiz, R. M. Bouse, *ibid.*, p. 1681.
40. S. B. Keith, *Ariz. Bur. Geol. Tech. Map 19* (1984); S. J. Reynolds *et al.*, *Ariz. Bur. Geol. Mines Tech. Bull. 197* (1986).
41. P. J. Coney and T. Harms, *Geology* **12**, 550 (1984); J. E. Spencer and S. J. Reynolds, *Ariz. Geol. Soc. Dig.* **17**, 539 (1989).
42. We report 1σ for Re-Os ages on the basis of inductively coupled plasma–mass spectrometry (ICP-MS) run statistics for each sample, with uncertainties typically better than 3%. Reproducibility is better than 1% on the spikes and better than 3% on replicate fusions and distillations. Uncertainties on all analytical procedures are equal to or better than the uncertainty in the half-life of ^{187}Re (4.23 ± 0.13 × 10^{10} years) (*43*).
43. M. Lindner *et al.*, *Geochim. Cosmochim. Acta* **53**, 1597 (1989).

44. We thank S. R. Titley and P. J. Coney for discussions and reviews, and two anonymous reviewers for their helpful comments. Supported by the National Science Foundation grant EAR-90123123, and by the W. M. Keck Foundation for the purchase of the TS-Sola ICP-MS.

Crystallization at Inorganic-Organic Interfaces: Biominerals and Biomimetic Synthesis

Stephen Mann,* Douglas D. Archibald, Jon M. Didymus, Trevor Douglas, Brigid R. Heywood,† Fiona C. Meldrum, Nicholas J. Reeves

Crystallization is an important process in a wide range of scientific disciplines including chemistry, physics, biology, geology, and materials science. Recent investigations of biomineralization indicate that specific molecular interactions at inorganic-organic interfaces can result in the controlled nucleation and growth of inorganic crystals. Synthetic systems have highlighted the importance of electrostatic binding or association, geometric matching (epitaxis), and stereochemical correspondence in these recognition processes. Similarly, organic molecules in solution can influence the morphology of inorganic crystals if there is molecular complementarity at the crystal-additive interface. A biomimetic approach based on these principles could lead to the development of new strategies in the controlled synthesis of inorganic nanophases, the crystal engineering of bulk solids, and the assembly of organized composite and ceramic materials.

Of the many challenges facing crystal science, the unification of molecular and mechanistic descriptions of crystal nucleation, growth, morphology, and dissolution is of pivotal importance. The dichotomy between the kinetic models of Burton, Cabrera, and Frank (*1*, *2*) and a molecular description of the structure, bonding, stereochemistry, and reactivity of crystal surfaces and nuclei has narrowed in recent years, but the disparity remains uncomfortably large. For example, the concept of order-disorder phase transformations in two-dimensional Ising lattices and the associated phenomenon of kinetic roughening have been extensively studied, yet we have little understanding of the consequences of such events on the molecular scale. For example, how do bond lengths, coordination environments, and nanoscale structure change during a roughening transition? The answers to such

The authors are in the School of Chemistry, University of Bath, Bath BA2 7AY, United Kingdom.

*To whom correspondence should be addressed.
†Present address: Department of Chemistry, University of Salford, Manchester M5 4WT, United Kingdom.

questions require a move away from the predominant kinetic paradigm of chemical engineers and physical chemists to a perception of crystal science in terms of bonding and reactivity of extended organized structures, that is, toward the view held by many synthetic chemists who use crystal structure data to explain the electronic and stereochemical properties of new compounds.

Some progress has been made, mainly in the field of organic solid-state chemistry (*3, 4*), in which the key structural and stereochemical factors associated with nucleation and crystal morphology can be more readily identified than in systems that are characterized by ionic bonding. The application of a molecular approach to inorganic materials has been essentially restricted to the geometric (epitaxial) models proposed many years ago by Whetstone (5) and Buckley (6) that were developed to explain the interaction of additives with specific crystal faces. Inorganic interfaces involved in oriented overgrowth have been treated from a similar perspective, and unit cell matching of close-packed structures can account for oriented nucleation, provided that the substrate and overgrowth have relatively simple lattice symmetries. However, although these models appear to be realistic descriptions of many simple phenomena, they have not provided adequate explanations for the processes that result in the controlled crystallization of inorganic solids in biological systems.

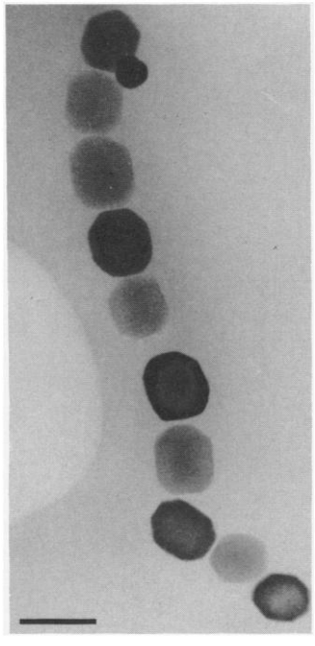

Fig. 1. Transmission electron micrograph showing a chain of discrete intracellular magnetite (Fe_3O_4) crystals. The crystals have well-defined particle sizes, are crystallographically oriented, and exhibit species-specific morphologies. Scale bar = 0.1 μm.

Crystal Science and Biomineralization

Biomineralization results in complex materials, such as bones, shells, and teeth, that are characterized by a remarkable level of molecular control of the particle size, structure, morphology, aggregation, and crystallographic orientation of the mineral phases (*7, 8*). Moreover, these biogenic minerals are in intimate association with organic polymers and macromolecules such that the products are of functional value as structural supports, mechanical devices, and sensors. This level of crystal engineering is not restricted to higher organisms but is characteristic of many simple organisms such as bacteria and protozoa (Fig. 1).

A central tenet of biomineralization is that the nucleation, growth, morphology, and aggregation (assembly) of the inorganic crystals are regulated by organized assemblies of organic macromolecules (the "organic matrix") (9). Control over the crystallochemical properties of the biomineral is achieved by specific processes involving molecular recognition at inorganic-organic interfaces (*10*). In this article, we review some of our recent experiments in which we model biomineralization and elucidate the role of molecular recognition in inorganic crystallization systems. We show how organized organic surfaces can control the nucleation of inorganic materials by geometric, electrostatic, and stereochemical complementarity between incipient nuclei and functionalized substrates. We also describe how analogous interactions are responsible for the morphological modification of inorganic crystals grown in the presence of anionic organic additives. Our aim is to highlight a molecular description of nucleation and growth that complements the more classical quantitative approach of physical chemistry. Moreover, a biomimetic approach based on molecular recognition at inorganic-organic interfaces could be useful in the synthesis of inorganic nanophases, bulk solids, and composite and ceramic materials (*11*).

Nucleation

How then, should we envisage inorganic nucleation in biological systems? We consider the formation of inorganic nuclei on the surface of an organic matrix to be analogous to an enzyme-substrate interaction in which the nuclei are kinetically stabilized by specific molecular interactions with the organic surface. In general, the effect of the organic substrate is to lower the activation energy of nucleation ($\Delta G^{\#}$). Moreover, $\Delta G^{\#}$ may be dependent on the two-dimensional structure of different crystal faces because each set of symmetry-related faces could exhibit a different level of complementarity with respect to the functionalized organic substrate. Indeed, we can consider these different interactions as corresponding to a series of activated clusters, each of different $\Delta G^{\#}$, such that there may be an ensemble of nucleation profiles that are crystallographically specific and dependent on the nature (degree of functionality, ionization, and structural assembly) of the organic matrix (Fig. 2).

What features of the inorganic nuclei can be recognized by the organic matrix? In principle, complementarity between the surface lattice geometries (including relaxation), spatial charge distributions, polarity of hydration layers, defect sites, and stereochemistries of the inorganic and organic surfaces are all possible. Unfortunately, there is a dearth of direct experimental evidence on the nature of these interfacial processes. Circumstantial evidence suggests that coordination environments in the mineral phase are simulated by metal-ion binding to appropriate ligands exposed at the organic surface. For example, carbonate and phosphate biominerals are often associated with carboxylate-rich (aspartate and glutamate) and phosphorylated (phospho-

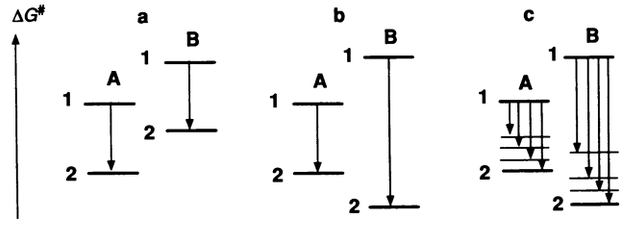

Fig. 2. Diagrammatic representation of the activation energies of nucleation, $\Delta G^{\#}$, of inorganic minerals in the absence (state 1) and presence (state 2) of an organic surface involved in biomineralization. Three possibilities exist for a mineral of two polymorphic structures (or two nucleation orientations), A and B, where A is the more kinetically favored in the absence of the organic matrix. (**a**) Nonspecific nucleation catalysis in which both polymorphs (or crystal faces) have reduced activation energies because of the presence of the matrix surface but there is no change in the outcome of mineralization. (**b**) Structure-specific nucleation of polymorph (or crystal face) B due to molecular recognition and high-fidelity synthesis or replication of the matrix surface. (**c**) Combination of (a) and (b) depending on the levels of recognition of nuclei A and B and the fidelity of matrix production, both of which may be influenced by genetic, metabolic, and environmental processes.

serine) proteins, respectively (9). The organic functional groups act as surrogate oxyanions that simulate the inorganic stereochemistry in the first layer of the incipient nuclei. Similarly, biominerals such as silica and ice, which contain polar $-OH$ or H_2O groups, are nucleated in association with hydroxy-rich macromolecules such as polysaccharides and proteins that contain high concentrations of serine and threonine residues (*12*, *13*). However, the interfacial recognition of the nearest neighbor interactions is not sufficient to generate the longer range translational symmetry of the inorganic lattice. This can only be achieved by control of the spatial disposition of functional groups across the matrix surface. Thus, the secondary, tertiary, and quaternary structures of assembled macromolecules are often key features of the preorganization required for controlled inorganic nucleation. Molecular periodicity can be attained by the use of β-pleated protein sheets (shells), α helices (fish antifreeze proteins), and organized phospholipid membranes. The construction of large-scale structures, such as shell and bone, relies on regiospecific nucleation in which active sites are spatially arranged over relatively long distances (micrometers). This is accomplished by cellular regulation of the synthesis, transport, and deposition of the matrix components and is under metabolic control.

Ferritin: Spatial charge and nucleation catalysis. The integration of organic supramolecular chemistry and inorganic crystallization is exemplified by the iron storage protein ferritin. This protein, which is present in bacteria, animals, and plants, consists of a spherical polypeptide shell that surrounds an inorganic core of the iron oxide mineral ferrihydrite. The system is effectively a nanoscale host-guest inorganic-organic assembly. The micelle is constructed from 24 polypeptide subunits arranged in cubic symmetry such that molecular channels penetrate the shell. The internal cavity is ~8 nm in diameter, which sets an upper limit of 4500 Fe atoms that can be accommodated in the mineral core. The structure of ferritin is complicated by the fact that there are two different subunits, designated H (heavy) and L (light) according to their relative molecular masses. Some ferritins, such as that isolated from horse spleen, are enriched (90%) in the L-chain subunit, whereas others, for example, the one from human heart, contain predominantly the H-chain subunit.

The difficulty of studying mineralization in heteropolymeric ferritins has been overcome by the ability to produce recombinant homopolymer ferritins (100% H or L subunits) (*14*), which can be crystallized and studied by x-ray diffraction (*15*). There is a specific metal-binding oxidation site in the H-chain but not in the L-chain polypeptide subunit (*15*). This site is close to an anionic patch of three glutamate residues on the inner surface of the protein shell (Fig. 3). Recently, we have undertaken experiments involving the in vitro mineralization of ferritins modified by site-directed mutagenesis to produce proteins depleted of the oxidation site or of cavity surface glutamates, or both (*16*). The data indicate that amino acid modifications in these residues result in reduced kinetics of iron oxide formation. Moreover, both sites act cooperatively in achieving the specific deposition of ferrihydrite within the protein cav-

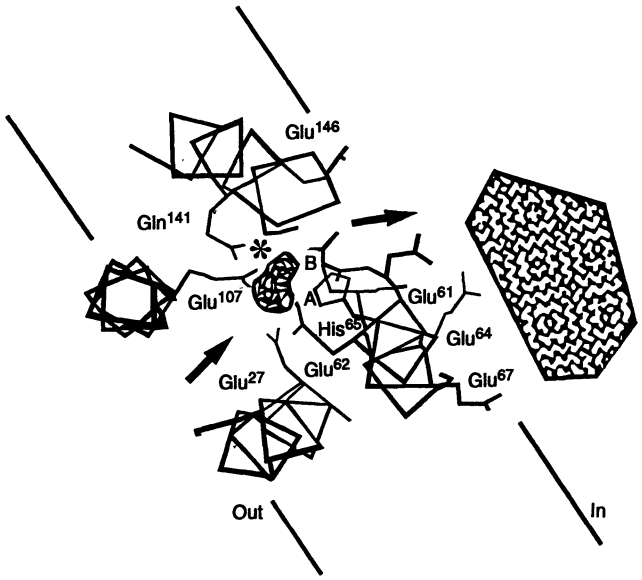

Fig. 3. Diagram showing the possible mechanism of iron oxide nucleation in ferritin. One polypeptide subunit is shown spanning the protein shell. The Fe(II) species, present in the external environment, bind at the ferroxidase center (*), where they undergo rapid oxidation. Migration of Fe(III) into the cavity results in mineral nucleation at a site comprising three glutamate residues. [Adapted from (*15*)]

Table 1. Oriented nucleation of inorganic crystals under Langmuir monolayers.

System	Monolayer	[Metal] (mM)	Mineral	Nucleated face
$CaCO_3$	$CH_3(CH_2)_{16}COO^-$	7–10	Calcite	$\{1\bar{1}0\}$
		4–6	Vaterite	(001)
	$CH_3(CH_2)_{17}NH_3^+$	4–10	Vaterite	(001) + (110)
	$CH_3(CH_2)_{19}OSO_3^-$	10	Calcite	(001)
	$CH_3(CH_2)_{19}PO_3^{2-}$	10	Vaterite	(001)
	$CH_3(CH_2)_{17}OH$	4–10	Calcite + vaterite	Nonoriented + inhibited
	$C_{27}H_{45}OH$*	4–10	Calcite	Nonoriented
$BaSO_4$	$CH_3(CH_2)_{19}OSO_3^-$	0.15	Barytes	(100)
	$CH_3(CH_2)_{19}PO_3^{2-}$	0.15	Barytes	(100)
	$CH_3(CH_2)_{19}COO^-$	0.15	Barytes	(010)
$CaSO_4$	$CH_3(CH_2)_{17}NH_3^+$	20–40	Gypsum	(010) + $\{\bar{1}03\}$
	$CH_3(CH_2)_{19}OSO_3^-$	20–40	Gypsum	(010) + $\{\bar{1}03\}$
	$CH_3(CH_2)_{19}PO_3^{2-}$	20–40	Gypsum	(010) + $\{\bar{1}03\}$
	$CH_3(CH_2)_{19}COO^-$	20–40	Gypsum	(010) + $\{\bar{1}03\}$
	$CH_3(CH_2)_{17}OH$	20–40	Gypsum	(010)

*Cholesterol.

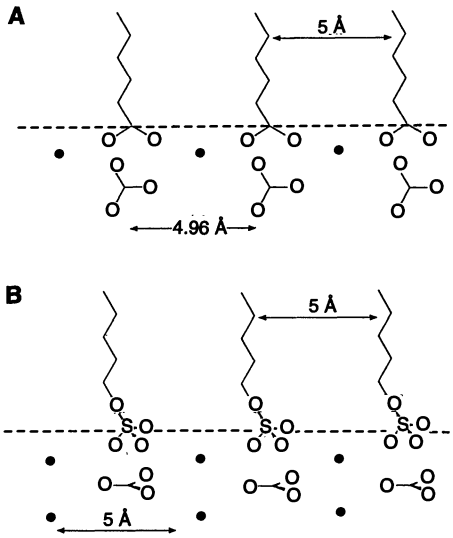

Fig. 4. Geometric and stereochemical complementarity at monolayer-crystal interfaces. (**A**) Nucleation of the calcite $\{1\bar{1}0\}$ face under carboxylate monolayers. (**B**) Nucleation of the calcite (001) face under sulfate monolayers.

ity. One possibility is that Fe(III) species formed at the ferroxidase center readily migrate into the cavity because of the electrostatic field of the neighboring glutamate residues located on the cavity surface. These residues, unlike the ligands of the ferroxidase site, are conserved in both H- and L-chain ferritin subunits and are putative nucleation sites.

These results indicate that nucleation specificity can be generated by the in situ production of ionic species [Fe(III)] that are subsequently accumulated in the presence of localized electrostatic fields. The effect is presumably to decrease the encounter time between collisions such that the critical radius can be readily surpassed. The process is very subtle because a change in a few amino acid residues at the appropriate sites in the protein markedly reduces the kinetic specificity of intraferritin nucleation. However, the level of molecular recognition in this system is limited to charge and polar interactions and hence is restricted to the short range. Thus, the nuclei are kinetically stabilized but not crystallographically oriented.

Surface recognition: Oriented nucleation on organized organic surfaces (Langmuir monolayers). One of the most striking aspects of biomineralization is the widespread phenomenon of oriented crystallization. For example, electron diffraction studies of partially demineralized mollusk shells have shown that in some species both the *a* and *b* axes of an antiparallel β-pleated sheet protein are aligned with the *a* and *b* crystallographic directions of aragonite ($CaCO_3$) (*17*). Partial amino acid sequencing of these acidic proteins (*18*) has indicated that there are repeated domains of polyaspartate, which could be the nucleation centers.

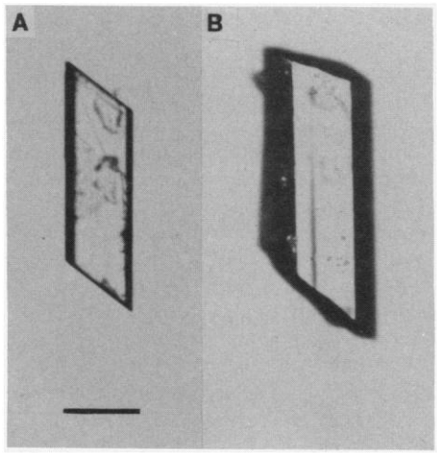

Fig. 5. Optical micrographs showing $CaSO_4 \cdot 2H_2O$ crystals nucleated under a compressed *n*-eicosyl sulfate monolayer. (**A**) Crystal nucleated on the (010) face; the *c* axis (long morphological axis) is aligned parallel to the monolayer surface. (**B**) Crystal nucleated on the $\{\bar{1}03\}$ end face; the crystal has been removed from the monolayer and is viewed along the *b* axis to show the asymmetry in the end faces arising from oriented nucleation. In situ, the long morphological axis is approximately perpendicular to the monolayer surface. Scale bar = 0.02 mm.

These suggestions are borne out by model systems in which calcite crystals have been grown on sulfonated polystyrene films with or without adsorbed polyaspartic acid (*19*). Rigid, highly sulfonated films induce the preferential nucleation of the calcite (001) face, and this effect is increased tenfold in the presence of adsorbed polyaspartate in the β-pleated sheet conformation. Interestingly, although oriented nucleation was observed, the nucleation density remained relatively low, suggesting that substrates capable of aligning nuclei may not necessarily be highly active as nucleation sites. Because the structures of these macromolecular surfaces are difficult to elucidate, we have chosen to study simpler organic substrates formed by compressing surfactant monolayers at the air-water interface of supersaturated solutions (*20–23*) (Table 1). Our results indicate that ion binding, lattice matching, and stereochemical recognition are important factors responsible for oriented nucleation. For example, Ca binding to negatively charged stearate ($C_{17}CO_2^-$) monolayers results in the nucleation of the $\{1\bar{1}0\}$ face of calcite (*24*) (Fig. 4). The pseudohexagonal net of stearate molecules has an interheadgroup spacing of ~0.5 nm, which matches the distance between coplanar Ca^{2+} on the $\{1\bar{1}0\}$ face. Similar geometric correspondences are present for the (100) face of $BaSO_4$ crystals nucleated under long-chain alkyl sulfate or phosphonate monolayers (*25, 26*). In addition to these geometric relations, the stereochemical arrangement of the surfactant headgroups is of fundamental importance. Nucleation of the calcite $\{1\bar{1}0\}$ face, for example, is favored by carboxylate headgroups because the bidentate motif mimics the carbonate stereochemistry exposed on this crystal surface; nucleation of the (001) face, on the other hand, is induced by sulfate headgroups because the tridentate arrangement simulates the oxygen positions of carbonate anions lying parallel to this crystal surface (Fig. 4) (*27*).

Similar experiments have been undertaken with the hydrated phase gypsum ($CaSO_4 \cdot 2H_2O$) (*27*). In the absence of a compressed monolayer, gypsum grew at the air-water interface in the form of randomly oriented, intergrown needles elongated along the *c* axis. Nucleation under negatively charged monolayers was enhanced, and the crystals were discrete and oriented with the *c* axis parallel or approximately perpendicular to the air-water surface (Fig. 5). Whereas the negatively charged headgroups (sulfate and phosphate) gave a 60:40 mixture of needles aligned normal and parallel to the monolayer, respectively, the polar surfactant octadecanol, although less effective at promoting nucleation, induced the nucleation of the (010) face such that essentially 100% of the gypsum needles were oriented with the *c* axis parallel to the monolayer surface. The (010) face lies parallel to the layers of water molecules in the unit cell and appears to be effectively stabilized by polar interactions with the hydroxyl headgroups of the octadecanol monolayer. Thus, although charge and stereochemical interactions are not selective in determining the orientation of the gypsum crystals, hydrogen bonding at the crystal-monolayer interface is an important aspect of nucleation. A similar effect has been observed with ice nucleation under long-chain alcohols (*28*).

Growth and Morphology

A perspective based on molecular recognition is expedient to the study of inorganic crystal growth. Although classical kinetic descriptions work well for simple ionic salts, we would like to understand how the reactivity of growth sites depends on molecular configuration rather than view the system as a hypothetical geometric array of (cubic) growth units. We, and others, have begun to probe the interaction of crystal surfaces with molecular-specific additives, and some of our recent data are described below. In general, it is clear that charge, geometry, and stereochemistry are important aspects of the crystal-additive interactions. Moreover, these interactions are dynamic such that specific changes in morphology probably originate from subtle differences in the kinetics of these recognition processes on different crystal faces rather than from high-affinity (irreversible) additive binding on one preferred set of symmetry-related surfaces.

Surface incarceration: Host-guest interfaces based on charge-size considerations. At the present time, there is much interest in the potential of host-guest interactions both in liquid systems involving supramolecular chemistry (such as cryptands) and in solid phases with layered or porous structures (intercalation compounds). In a sense, a growing crystal face represents the ultimate host because not only does it readily accommodate soluble guests (growth units) but also it quickly enrolls them as new members (hosts) of the expanding surface. In the presence of extraneous additives, however, the role of the crystal surface is more analogous to the conventional view of host-guest systems. In such cases, the surface layers of the crystal can incorporate soluble

additives provided there is a degree of complementarity in charge and size between the guest ions and interstices in the structure of the crystal boundary layers.

Two possibilities can arise. First, the additive is incarcerated in the hydrated, relaxed surface structure but is excluded from the bulk. The crystal is then covered by a host-guest layer that is in steady state with the development of the growth fronts at the crystal-solution interface. A preferential distribution of the incarcerated ions on certain crystal faces can result in morphological changes because of reductions in symmetry or structural stabilization, or both, which result in differential kinetics. Second, the additive is accommodated as an integral part of both the surface and the bulk structures of the growing crystals (a host-hostage phase?). Occlusion is probably favored when there is only marginal difference between the surface and bulk structures. Changes in the unit cell parameters and in crystal symmetry and morphology and the adoption of superstructures are possible consequences of solid-solution behavior.

Simple cations and anions can exert profound influences on the morphology of inorganic crystals. Recently, Rajam and Mann have shown that Li^+ has a dramatic effect on the shape of calcite crystals (*29*). In the presence of relatively high Li^+ concentrations (Ca:Li = 1:10), the rhombohedral {104} faces of calcite become truncated by well-defined basal (001) surfaces, resulting in hexagonal tabular crystals. No changes in bulk structure are observed by high-resolution x-ray powder diffraction, suggesting that the morphological change is due to surface interactions alone. The relatively high Li^+ concentrations required for this effect suggest a specific electrostatic shielding of the (001) face due to Li^+ located in surface sites. In particular, the net dipole moment present on this face can be effectively neutralized by Li^+ intercalation into vacant tetrahedral holes without significant surface reconstruction. A theoretical examination of this system used an approach based on the atomistic simulation of inorganic surfaces (*30*). In this approach, the surface structure and stability and the effect of impurities on surface energy are calculated for different crystal faces. Provided that an accurate parametrization of the force field can be determined, morphological changes in the presence of additives can be predicted. In this way, Titiloye *et al.* have shown that, whereas Mg^{2+} stabilizes the $\{1\bar{1}0\}$ faces of calcite, Li^+ interacts specifically with the basal (001) faces (*31*). Development of these theoretical procedures to accommodate the interaction of more complex additives such as HPO_4^{2-} with calcite surfaces has been undertaken (*32*).

Surface recognition: Spatial charge and stereochemical requirements. Low molecular weight additives that have molecular structures with variable conformational states will interact with inorganic crystal surfaces through electrostatic and stereochemical processes. For example, α-ω-dicarboxylic acids $[(CH_2)_n(CO_2H)_2]$ are effective at stabilizing the $\{1\bar{1}0\}$ faces of calcite provided that both carboxylate groups are ionized and $n < 3$ (*33*). Carbonate is incorporated into these faces by bidentate binding to Ca^{2+}, and this effect can be simulated by the dicarboxylate interactions if the spacing between the ligands is close to 0.4 nm. Both malonate and maleate fit this criterion, but the increased rigidity of the latter reduces the binding affinity. Similar effects have been observed for $BaSO_4$ crystals grown in the presence of diphosphonates (*34*).

Charge functionalization of additives can enhance their morphological specificity; for example, both α-aminosuccinate (aspartate) and γ-carboxyglutamate show more effective stabilization of the prismatic calcite $\{1\bar{1}0\}$ faces than succinate or glutamate, respectively (*33*). Increasing the hydrophobicity of the additive, however, generally reduces its ability to induce morphological changes during crystallization. Thus, whereas butyl phosphate binds specifically to calcite $\{4\bar{4}1\}$ faces, naphthyl phosphate is ineffective (*35*).

In other experiments, different morphological effects can be induced by seemingly marginal changes in the molecular structure of the additive; for example, whereas prismatic calcite crystals are formed in the presence of phenyl phosphate, phenyl phosphonate produces crystals of unusual rhombohedral form (Fig. 6). A possible explanation for this remarkable difference is that rotation of the phenyl ring about the C–O–P linkage of phenyl phosphate enables the molecule to bind in an orientation complementary to the carbonate stereochemistry of the $\{1\bar{1}0\}$ prismatic faces. However, this is not an acceptable orientation for the phenyl phosphonate molecule because the aromatic ring would be very close to the charged crystal surface as a result of the presence of the C–P bond. Clearly, when one begins to consider the stereochemical possibilities of macromolecular interactions with inorganic crystal faces, then the recognition processes can become extremely complex. However, studies have shown that acidic macromolecules extracted from sea urchin tests interact specifically with calcite prismatic faces (*36*), suggesting that the acidic amino acid carboxylate groups behave in a stereochemical fashion similar to that observed with the low molecular weight dicarboxylate additives.

Solution chemistry and reactivity. Any discussion of the structural and stereochemical influence of organic additives on the crystal morphology of inorganic materials should be framed within the physicochemical context of the crystallization system. In this regard, speciation is particularly important because the basis of recognition depends on the precise transfer of molecular information at the crystal-additive interface. Systems in which there is a range of equilibria involving chemically variant species can be subject to radical changes in morphology depending on such factors as pH, ionic strength, and complexation (*37*). Moreover, these equilibria may fluctuate during the course of the crystallization reaction such that time-dependent morphologies can be obtained.

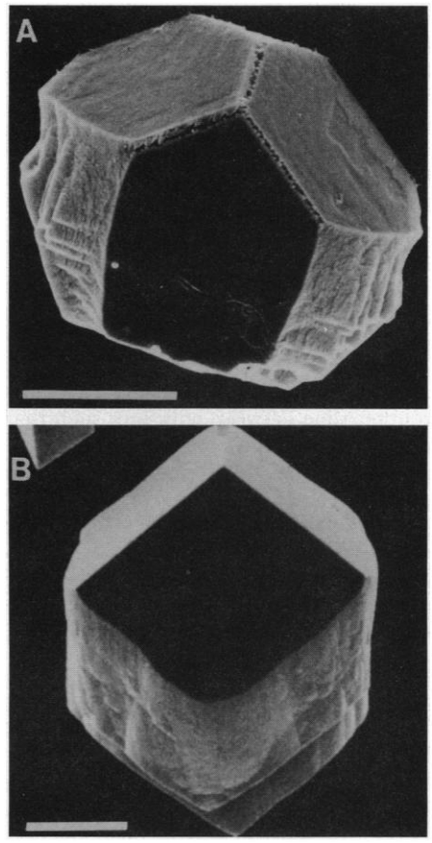

Fig. 6. Scanning electron micrographs of calcite crystals grown in the presence of (**A**) phenyl phosphonate and (**B**) phenyl phosphate. Scale bars = 10 μm.

More complicated situations arise when crystallization is associated with phase transformations involving chemical reactions. In such cases, it is unlikely that even an approach that combines structural, stereochemical, and kinetic considerations is sufficient, and only an understanding of chemical reactivity will suffice. For example, the crystal growth of iron oxides, such as Fe_3O_4 and Fe_2O_3, from aqueous solution involves surface reactions such as ligand exchange, hydrolysis, proton loss, and oligomerization,

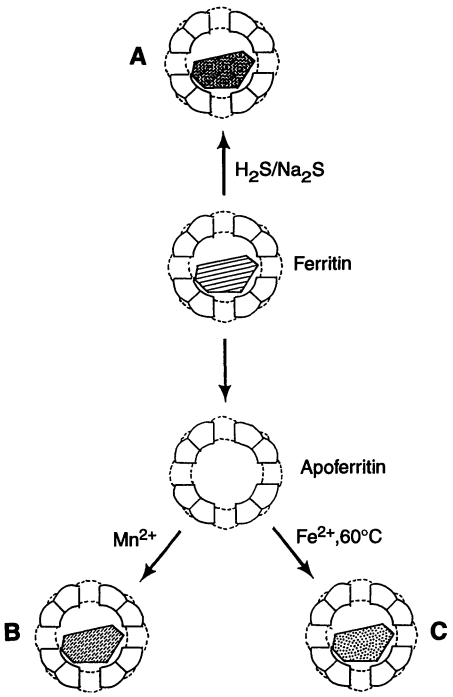

Fig. 7. The use of supramolecular protein cages (ferritin) in the synthesis of nanophase inorganic materials. The products are (A) iron sulfide, (B) manganese oxide, and (C) magnetite (Fe_3O_4).

all of which could be influenced by organic molecules. Moreover, it is probable that in such cases the crystals grow through a hydrated pseudocrystalline surface-oxide interphase such that the chemistry of phase transformation needs to be understood.

A relatively new approach to understanding the structure and reactivity of complex systems involves the theoretical modeling of the complexation and hydrolysis behavior of species using a partial charge model based on the equalization of electronegativity (*38*). This method can be used to calculate the expected degree of interaction between a growth additive and aqueous species before nucleation. For example, complexation versus pH diagrams can be obtained for additives with straight-chain precursors of general formula $[Fe_x(H_2O)_{y-h}(OH)_h]^{3x-h}$ (where x is varied from 1 to 10 and $y = 4x + 2$) (*39*). The calculations show that at pH = 2 both phosphate and sulfate complex strongly with multinuclear Fe(III) complexes and hence perturb the crystal morphology of hematite, as confirmed by experimental results (*39*). Phosphate esters, on the other hand, have stability fields that lie outside the experimental pH and show marginal morphological effects.

The partial charge model can also be used to determine the relative labilities of complexed iron(III) precursors ($[Fe(H_2O)_2(OH)_2X]^0$, where X is a complexing anionic species) toward oxolation and complete hydrolysis (*39*). Oxolation can be considered as a 1,3 prototropic shift from OH to H_2O, and the calculated partial charge on H_2O [$\delta(H_2O)$] predicts whether this shift is reversible or not and hence whether oxolation and complete hydrolysis (oxide formation) is favored over olation (oxyhydroxide formation). The calculated partial charges, $\delta(H_2O)$, become more positive as the electronegativity of the anionic additive increases as a result of inductive effects at the metal center. For inorganic oxyanions, the values are positive [for example, for H_2PO_4, $\delta(H_2O) = +0.11$], implying that the Fe–OH_2 group is more acidic in the presence of the complexing anion and that oxide (hematite) formation is favored. In contrast, organic monophosphates gave negative $\delta(H_2O)$ values, predicting incomplete oxolation and nucleation of hydroxyoxide phases such as lepidocrocite (γ-FeOOH). These predictions were confirmed by experimental studies (*39*).

Biomimetic Approaches

The adaptation of ideas and concepts derived from biomineralization research to the synthesis of inorganic materials with controlled properties appears to be a promising area of investigation (*11*). In particular, processes that utilize supramolecular assemblies and control interfacial chemistry by molecular recognition could provide new routes to inorganic materials that exhibit uniform particle size (often nanoscale), polymorph selectivity, tailored morphology, oriented nucleation, organized assembly, and composite structures (organoceramics).

Organic cages and the synthesis of inorganic materials. The possibility of using host-guest systems to confine the synthesis of inorganic materials to small reaction volumes has been recently explored. Clearly, the required cavities are an order of magnitude larger than those provided by conventional hosts such as crown ethers and cyclodextrins. Zeolites offer some exciting prospects in synthesizing and immobilizing discrete inorganic clusters [such as CdS (*40*)], but the channel dimensions are usually well below 1.5 nm and the reaction products cannot be readily extracted from the host lattice. More versatility can be provided by organic supramolecular hosts such as reverse micelles and phospholipid vesicles because the size range of reaction environments (1 to 100 nm) is more extensive and there is the potential for molecular engineering of the surface functional groups. A range of nanometer-dimension inorganic materials [such as Ag_2O (*41*), Fe_3O_4 (*42*), calcium phosphates (*43*), Al_2O_3 (*44*), and CdS (*45*)] have been prepared within phospholipid vesicles. As each particle is surrounded by a bilayer membrane 4.5 nm thick, particle-particle interactions are negligible and reaction rates can be diffusion controlled. For example, slow membrane diffusion of OH^- into Fe(II)-loaded phosphatidylcholine vesicles results in the intravesicular crystallization of Fe_3O_4 compared with γ-FeOOH deposition under analogous conditions in bulk solution (*42*).

One problem encountered with the use of phospholipid or surfactant assemblies is their sensitivity to changes in phase behavior. Furthermore, the dynamic behavior of reverse micelles restricts their use in the synthesis of inorganic materials because the primary particles readily aggregate. To alleviate some of these difficulties, we have used more robust systems such as the mineral-free protein shell of ferritin (Fig. 7). The similar redox and aqueous chemistries of Mn(II)/(III) and Fe(II)/(III) have been utilized in the room-temperature synthesis of nanophase Mn(III) oxides within the 8-nm internal cavity of the protein shell (*46*). The resulting particles are uniform in size and monodisperse. Furthermore, because the protein can tolerate pH values up to 9.5 and temperatures of 60° to 80°C for limited periods, there is the possibility of extending the scope of this approach. For instance, Meldrum *et al.* have recently reported a synthetic route to the in situ deposition of Fe_3O_4 within the ferritin cage (*47*). The magnetic properties of this biocompatible ferrimagnetic protein are being explored, particularly in light of the possible use of such a system in magnetic imaging.

Organized organic surfaces and template mineralization. We have already described how organized monolayers of surfactant molecules can induce the oriented nucleation of inorganic crystals by recognition processes at the inorganic-organic interface. We know that changes in headgroup charge, packing, and stereochemistry bring about profound effects on the crystal chemistry. As yet, only a handful of inorganic materials have been studied [$CaCO_3$ (*21*), $BaSO_4$ (*22*), $SrSO_4$ (*48*), ice (*28*), NaCl (*49*), CdS (*50*), and PbS (*51*)], and further work is required to determine the general applicability of this experimental system.

A further possibility is to extend the two-dimensional organization of monolayers into three dimensions by utilizing the ability of certain chiral lipids to self-assemble into microstructures with high axial ratios. For example, helical ribbons can be prepared from diacetylenic phosphatidylcholine and subsequently coated with aluminum hydroxide (*52*). However, these mineralization reactions are nonspecific, probably because metal-ion binding is relatively weak as a result of the presence of strong interheadgroup interactions within the rigid crystalline lipid assembly. Increased specificity can be obtained by using rolled-up multilamellar

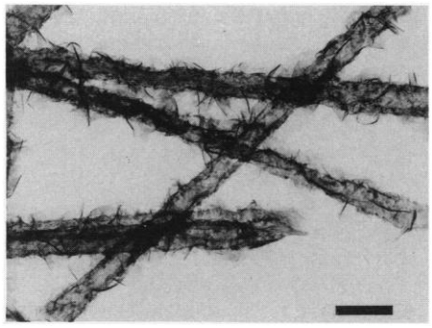

Fig. 8. Transmission electron micrograph of lipid galactocerebroside tubules coated with iron oxide. The lipid microstructures are doped with an anionic sulfated galactocerebroside, which promotes specific nucleation of the inorganic material on the surface of the organic supramolecular fiber. Scale bar = 300 nm.

cylinders of uncharged galactocerebrosides (*53*), which are tailored for inorganic nucleation by the inclusion of small amounts of anionic (sulfated) galactocerebroside molecules. Under appropriate solution conditions, these doped microstructures act as specific nucleation templates for iron oxide mineralization (*54*) (Fig. 8). Moreover, the organomineral fibers can undergo in situ chemical transformations, for example, to produce magnetic fibers coated in the mineral magnetite (Fe_3O_4).

In a related approach organic polymers containing functional surface groups are used as active substrates for crystal nucleation (*55*). Epoxidation of styrene-butadiene copolymers appears to be a useful method because a range of functionalized polymers can be prepared by ring opening on the addition of various acids. A related strategy involves the use of unfunctionalized and functionalized poly(organosiloxane) surfaces in promoting calcite nucleation (*56*). In general, the advantage of using polymeric systems is that a range of chemical modifications is readily available through relatively straightforward organic chemistry. The disadvantage of these systems, unlike surfactant assemblies, is that the structure of the functionalized surfaces is often difficult to characterize.

Conclusions

The adaptation of biomineralization processes in the laboratory highlights the potential of a biomimetic approach to crystal science. In particular, the concept of molecular recognition at inorganic-organic interfaces involved in nucleation and crystal growth is providing a perspective in which the classical approaches to inorganic crystallization can be developed within a structural and stereochemical context. Moreover, the integration of organic supramolecular chemistry, self-assembly, and inorganic materials chemistry provides the opportunity to develop rational synthetic routes to products with uniform particle sizes, nanoscale dimensions, tailored morphologies, crystallographic orientation, and organized microarchitectures.

A key breakthrough will be the incorporation of molecular biology into inorganic materials science. For example, the precision of recombinant DNA technology in producing site-directed amino acid modifications has been invaluable in determining the nucleation and oxidation sites in the Fe storage protein ferritin (*15*, *16*). New mutants could be constructed with the objective of tailoring the ligand chemistry to nonnative minerals, for example, CdS. More generally, the genetic production of functionalized biopolymers containing extended motifs of periodic metal-ion binding sites, such as charged β-pleated sheets, could be a possible route to the reproducible fabrication of organized organic substrates for use in the synthesis of inorganic materials. Clearly, an interdisciplinary approach of this magnitude relies on the unlocking of our imagination from the confines of conventional disciplines. A new paradigm is imminent.

REFERENCES AND NOTES

1. W. K. Burton and N. Cabrera, *Discuss. Faraday Soc.* **5**, 33 (1949).
2. _____, F. C. Frank, *Philos. Trans. R. Soc. London Ser. A* **243**, 229 (1951).
3. I. Weissbuch, L. Addadi, M. Lahav, L. Leiserowitz, *Science* **253**, 637 (1991).
4. E. M. Landau *et al.*, *J. Am. Chem. Soc.* **111**, 1436 (1989).
5. J. Whetstone, *Discuss. Faraday Soc.* **16**, 132 (1954).
6. H. E. Buckley, *ibid.* **5**, 243 (1949).
7. S. Mann, J. Webb, R. J. P. Williams, Eds. *Biomineralization: Chemical and Biochemical Perspectives* (VCH Verlagsgesellschaft, Weinheim, Germany, 1989).
8. H. A. Lowenstam and S. Weiner, *On Biomineralization* (Oxford Univ. Press, Oxford, 1989).
9. S. Weiner, *Crit. Rev. Biochem.* **20**, 365 (1986).
10. S. Mann, *Nature* **332**, 119 (1988).
11. A. H. Heuer *et al.*, *Science* **255**, 1098 (1992); S. Mann *et al.*, *Mater. Res. Soc. Bull.* **17**, 32 (1992).
12. D. M. Swift and A. P. Wheeler, *J. Phycol.* **28**, 202 (1992).
13. P. K. Wolber and G. J. Warren, *Trends Biochem. Sci.* **14**, 179 (1989).
14. L. Levi *et al.*, *J. Biol. Chem.* **263**, 18086 (1988).
15. D. M. Lawson *et al.*, *Nature* **349**, 541 (1991).
16. V. J. Wade *et al.*, *J. Mol. Biol.* **221**, 1443 (1991).
17. S. Weiner and W. Traub, *Proc. R. Soc. London Ser. B* **304**, 425 (1984).
18. K. W. Rusenko, J. E. Donachy, A. P. Wheeler, *ACS Symp. Ser.* **444**, 107 (1991).
19. L. Addadi, J. Moradian, E. Shay, N. G. Maroudas, S. Weiner, *Proc. Natl. Acad. Sci. U.S.A.* **84**, 2732 (1987).
20. S. Mann, B. R. Heywood, S. Rajam, J. D. Birchall, *Nature* **334**, 692 (1988).
21. S. Mann, B. R. Heywood, S. Rajam, J. B. A. Walker, *J. Appl. Phys.* **24**, 154 (1991).
22. B. R. Heywood and S. Mann, *Adv. Mater.* **4**, 278 (1992).
23. S. Rajam, B. R. Heywood, S. Mann, *J. Chem. Soc. Faraday Trans.* **87**, 727 (1991).
24. B. R. Heywood, S. Rajam, S. Mann, *ibid.*, p. 735.
25. B. R. Heywood and S. Mann, *J. Am. Chem. Soc.* **114**, 4682 (1992).
26. _____, *Langmuir* **8**, 1492 (1992).
27. S. Mann, T. Douglas, B. R. Heywood, unpublished observations.
28. M. Gavish, R. Popovitz-Biro, M. Lahav, L. Leiserowitz, *Science* **250**, 973 (1990).
29. S. Rajam and S. Mann, *J. Chem. Soc. Chem. Commun.* **1990**, 1789 (1990).
30. M. J. Davies *et al.*, *J. Chem. Soc. Faraday Trans. 2* **85**, 555 (1990).
31. J. O. Titiloye, S. C. Parker, D. J. Osguthorpe, S. Mann, *J. Chem. Soc. Chem. Commun.* **1991**, 1494 (1991).
32. J. O. Titiloye, S. C. Parker, S. Mann, *J. Cryst. Growth*, in press.
33. S. Mann, J. M. Didymus, N. P. Sanderson, B. R. Heywood, E. J. Aso Samper, *J. Chem. Soc. Faraday Trans. 1* **86**, 1873 (1990).
34. R. J. Davey *et al.*, *Nature* **353**, 549 (1991).
35. J. M. Didymus *et al.*, *J. Chem. Soc. Faraday Trans.*, in press.
36. A. Berman, L. Addadi, S. Weiner, *Nature* **331**, 546 (1988).
37. E. Matijevic, *Chem. Mater.* **5**, 412 (1993).
38. J. Livage, M. Henry, C. Sanchez, *Prog. Solid State Chem.* **18**, 259 (1988).
39. N. J. Reeves and S. Mann, *J. Chem. Soc. Faraday Trans. 1* **87**, 3875 (1991).
40. N. Herron *et al.*, *J. Am. Chem. Soc.* **111**, 530 (1989).
41. S. Mann and R. J. P. Williams, *J. Chem. Soc. Dalton Trans.* **1983**, 311 (1983).
42. S. Mann, J. P. Hannington, R. J. P. Williams, *Nature* **324**, 565 (1986).
43. B. R. Heywood and E. D. Eanes, *Calcif. Tissue Int.* **41**, 192 (1987).
44. S. Bhandarkar and A. Bose, *J. Colloid Interface Sci.* **135**, 531 (1990).
45. H.-C. Youn, S. Baral, J. H. Fendler, *J. Phys. Chem.* **92**, 6320 (1988).
46. F. C. Meldrum, V. J. Wade, D. L. Nimmo, B. R. Heywood, S. Mann, *Nature* **349**, 684 (1991).
47. F. C. Meldrum, B. R. Heywood, S. Mann, *Science* **257**, 522 (1992).
48. N. P. Hughes, D. Heard, C. C. Perry, R. J. P. Williams, *J. Phys. D* **24**, 146 (1991).
49. E. M. Landau, R. Popovitz, M. Levanon, L. Leiserowitz, M. Lahav, *Mol. Cryst. Liq. Cryst.* **134**, 323 (1986).
50. X. K. Zhao, S. Xu, J. H. Fendler, *Langmuir* **7**, 520 (1991).
51. X. K. Zhao, J. Yang, L. D. McCormick, J. H. Fendler, *J. Phys. Chem.* **96**, 9933 (1992).
52. J. S. Chappell and P. Yager, *J. Mater. Sci. Lett.* **11**, 633 (1992).
53. D. D. Archibald and P. Yager, *Biochemistry* **31**, 9045 (1992).
54. D. D. Archibald and S. Mann, *Nature*, in press.
55. P. A. Bianconi, J. Lin, A. R. Strzelecki, *ibid.* **349**, 315 (1991); E. Dulas, *J. Mater. Chem.* **1**, 473 (1991); P. D. Calvert, *Mater. Res. Soc. Bull.* **17**, 37 (1992).
56. B. J. Brisdon, B. R. Heywood, A. G. W. Hodson, S. Mann, K. W. Wong, *Adv. Mater.* **5**, 49 (1993).

57. We thank P. M. Harrison, P. Arosio, S. Levi, and V. J. Wade for collaborative work on ferritin, S. Rajam for studies on calcite morphology, and the Science and Engineering Research Council, United Kingdom, and BP Research, United Kingdom, for financial support.